



# Assessing the environmental benefits of design for disassembly in buildings with a time-resolved prospective LCA approach

Haitham Abu-Ghaida<sup>1,2,3</sup> · Alexander Hollberg<sup>3</sup> · Michiel Ritzen<sup>2,4</sup> · Anna Wöhler<sup>3</sup> · Sebastien Lizin<sup>1,2</sup>

Received: 31 March 2025 / Accepted: 31 July 2025  
© The Author(s) 2025

## Abstract

**Purpose** This study advances building LCA methodology by introducing time-resolved prospective LCA (trP-LCA). This approach improves upon static LCA through both the integration of projected changes in background LCI data as well as the consideration of product recovery potential following Abu-Ghaida et al. (2024). We quantify differences between static and time-resolved approaches and assess whether embodied greenhouse gas (GHG) benefits of Design for Disassembly (DfD) remain sizable across various future scenarios.

**Methods** The trP-LCA method generates lifecycle inventories for each building product over its use timeline, including construction, replacement cycles, and end-of-life. We forecast inventory databases across nine scenarios, interpolating in 5-year increments for higher resolution temporal mapping. This methodology is applied to a case study of a single-family zero-energy building in the Netherlands, comparing three design variants: a business-as-usual design with conventional DfD elements, a variant with high disassembly potential, and one with minimal disassembly considerations.

**Results and discussion** Our results indicate that for the zero-energy building case study, static LCA (excluding Module D benefits) overestimates embodied GHG emissions by up to 32% relative to trP-LCA, with discrepancies increasing over the building's lifespan. Enhanced disassembly potential consistently reduces embodied emissions by 12 – 25% across all projected future scenarios. Module D benefits for material recovery exhibit counterintuitive trends; as production processes become cleaner in sustainable scenarios, the environmental burden of the avoided virgin production diminishes, thus reducing the calculated credit. These findings underscore that static LCA fails to capture the technological improvements over time, leading to inflated emission estimates, particularly for replacements produced decades after construction.

**Conclusions** Incorporating product recovery potential, trP-LCA yields substantially different impact estimates than static LCA for long-lived buildings, especially in replacement and end-of-life phases. Although the absolute benefits of DfD may shrink in greener futures, the relative advantages persist across all scenarios. Our study contributes to sustainable building design by providing a dynamic framework that informs designers and policymakers about long-term environmental impacts, thereby supporting the transition to low-carbon, resource-efficient built environments.

**Keywords** Time-resolved prospective LCA · Design for disassembly · Embodied carbon · Buildings · Circular economy · Prospective LCA · Product recovery potential

Communicated by Alexander Passer.

✉ Haitham Abu-Ghaida  
haitham.ghaida@uhasselt.be

<sup>1</sup> Centre for Environmental Sciences (CMK), UHasselt, Agoralaan, 3590 Diepenbeek, Belgium

<sup>2</sup> Energyville, Thor Park 8310, 3600 Genk, Belgium

<sup>3</sup> Department of Architecture and Civil Engineering, Division of Building Technology, Chalmers University of Technology, Sven Hultins Gata 6, 412 96 Göteborg, Sweden

<sup>4</sup> Unit Water and Energy Transition, VITO, Boeretang 200, 2400 Mol, Belgium

## 1 Introduction

The building sector is pivotal in global sustainability efforts, accounting for approximately 34% of global energy consumption and 37% of energy and process-related greenhouse gas (GHG) emissions (UN Environment Programme 2024). As the industry strives to meet ambitious decarbonization targets for 2050 (European Commission 2021; International Energy Agency 2021), attention is shifting from operational to embodied GHG emissions. These embodied emissions, arising from the production, replacement, transport, and

end-of-life (EoL) treatment of building materials, represent 21% of a building's lifecycle GHG emissions on average (Röck et al. 2020) and are projected to dominate total life-cycle emissions in highly energy-efficient structures (Anand And Amor 2017).

Life Cycle Assessment (LCA) has emerged as a crucial tool for quantifying the environmental impacts of buildings throughout their lifespan (Buyle et al. 2013). However, traditional LCA approaches face limitations in capturing the dynamic nature of technological progress, policy changes, and evolving energy systems (Frischknecht And Stucki 2010; Pauliuk et al. 2017; Voglhuber-Slavinsky et al. 2022).

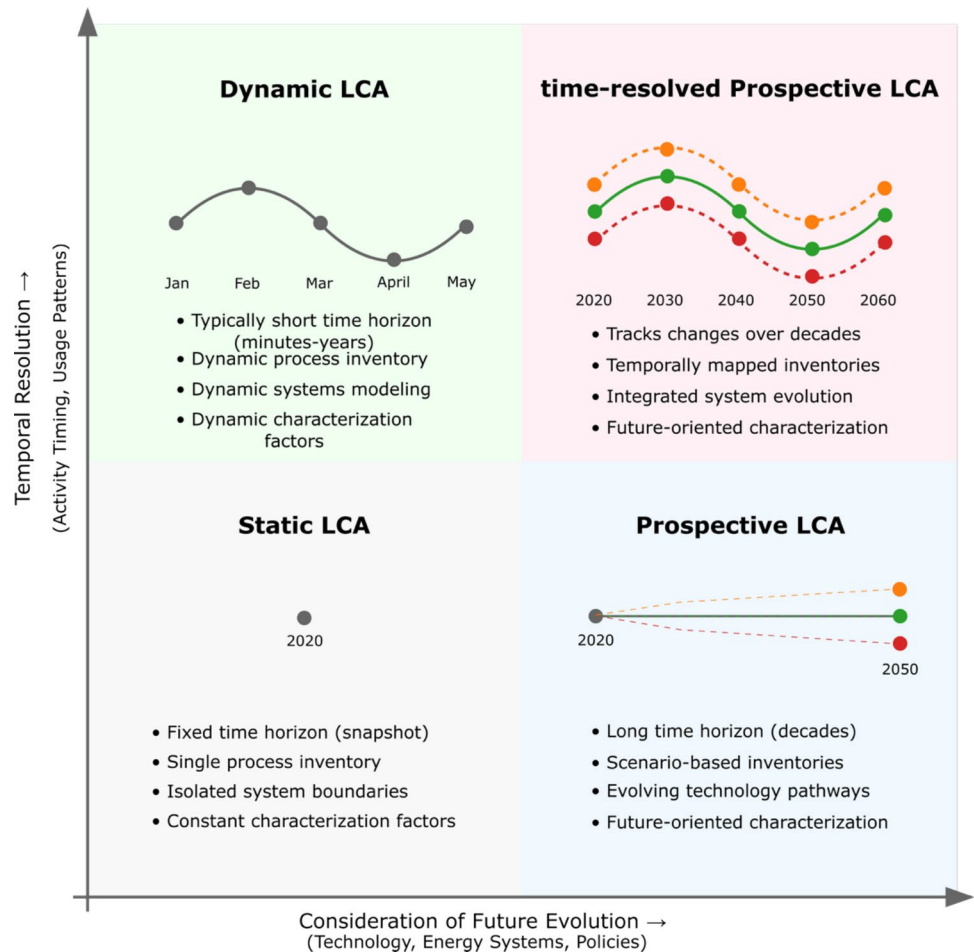
These limitations are particularly pronounced when assessing long-lived structures such as buildings, where impacts can vary significantly over time (Van de moortel et al. 2022; Fnais et al. 2022). Traditional LCA is especially ill-suited for evaluating the full potential of circular economy principles, which are inherently time-dependent. The benefits of strategies such as Design for Disassembly (DfD), for instance, are realized at a building's use and end-of-life, under technological and economic conditions that may be vastly different from today. The same challenge applies to other key circular strategies: the value of durability and

service life extension is determined by the environmental cost of the future replacements it avoids; the benefits of adaptability and flexibility are realized when a building is modified decades after construction, preventing emissions from demolition and new builds.

To address these temporal dimensions, LCA methodologies can be broadly categorized into three approaches: static, dynamic, and prospective. While these share foundational principles, they differ significantly in their treatment of time and future projections (Arvidsson et al. 2018; Cucurachi et al. 2022). Figure 1 illustrates the key differences between these approaches and our proposed trP-LCA method.

Static LCA, as standardized in ISO 14040, aggregates all environmental impacts to a single point in time, regardless of when they occur during a product's life cycle. This approach neither accounts for temporal emission variations nor considers background system changes over time. Dynamic Life Cycle Assessment (DLCA) incorporates time-dependent variations in inventory flows and characterization factors, though our study focuses only on dynamic inventories to specifically isolate the impact of evolving background technologies. This approach particularly enhances the assessment of climate change impacts,

**Fig. 1** Comparison of LCA approaches and their temporal treatment of environmental impacts. Static LCA (bottom left) aggregates all impacts to a single reference point, regardless of when they occur. DLCA (top left) captures temporal variations by tracking high-resolution impacts within the assessment period. Based on different scenarios, PLCA (bottom right) projects impacts at future points. trP-LCA (top right) combines temporal tracking with scenario evolution, mapping specific impacts to their occurrence time while accounting for changing background systems



where emission timing significantly affects environmental consequences (Levasseur et al. 2010). In building applications, for example, DLCA has been used to capture hourly fluctuations in grid carbon intensity (Roux et al. 2017) and time-dependent biogenic carbon fluxes (Pittau et al. 2022). Prospective Life Cycle Assessment (PLCA) focuses on evaluating emerging technologies and future scenarios, incorporating technological learning curves and market development projections (Cucurachi et al. 2018). PLCA scenarios typically combine Shared Socioeconomic Pathways (SSPs) with Representative Concentration Pathways (RCPs) to explore different future trajectories, from sustainable development (SSP1) to fossil-fueled growth (SSP5) (van Vuuren et al. 2017).

Building on these concepts, this study introduces time-resolved Prospective LCA (trP-LCA) as a methodological framework that combines the temporal tracking of inventory changes from DLCA with the future-oriented scenario analysis of PLCA. The concept of “time-resolved LCA” was first introduced by Zimmermann et al. (2014) as a middle ground between static and fully dynamic methods. In our application, trP-LCA maps life cycle inventory (LCI) data to specific points in time using projections from integrated assessment models (IAMs), which we generate using the PRospective EnvironMental Impact asSEssment (PREMISE) framework (Sacchi et al. 2022). This allows each process, product, or service’s environmental impact to be calculated using inventory data appropriate for its year of occurrence, emphasizing how technological evolution and system changes affect life cycle inventories over time.

This paper builds on our previous work, which introduced an LCA method for assessing product recovery potential in building LCAs using a disassembly network-based approach (Abu-Ghaida et al. 2024). While our previous research evaluated the environmental benefits of DfD for a Zero-Energy Building (ZEB) by accounting for product dependencies, it was limited by its static nature. The current study enhances this approach by incorporating projected changes in LCI data over time, integrating different combinations of SSPs and RCPs.

This research has two primary aims: (1) to determine whether the environmental benefits of DfD principles remain sizable across various future development pathways and (2) to quantify the differences in environmental impact estimates between conventional static LCA and trP-LCA when assessing building embodied emissions. To test our framework, we apply it to a building case study to quantify the embodied GHG emissions of three design variants with varying levels of disassembly potential: a business-as-usual (BAU) design, a high disassembly potential (HDP) design, and a low disassembly potential (LDP) design. By analyzing these variants across multiple future scenarios, we can assess the robustness of DfD benefits over time.

The contribution of this research lies in three key aspects: (1) it represents the first application of trP-LCA to buildings, (2) it is the first study to assess circular economy principles, specifically DfD, by using a time-resolved approach, and (3) it extends the application of the PREMISE framework to building component lifecycles, demonstrating how prospective LCI data can inform circular economy strategies in the built environment.

This methodological approach is particularly relevant for long-term infrastructure assessment, where both temporal considerations and future projections play essential roles. By tracking how LCI data evolves over time while incorporating different development pathways, the framework provides insights into how building design choices affect environmental performance under different future conditions. A significant research gap exists regarding the temporal robustness of circular design strategies. As background systems evolve toward decarbonization, the environmental advantage of strategies such as DfD may theoretically diminish due to the decreasing emissions intensity of production processes. This research systematically examines this methodological question by quantifying the relative benefits of enhanced disassembly potential across divergent future pathways, addressing what Fnais et al. (2022) identified as a critical need in building LCA: the integration of temporal information in lifecycle inventories.

The paper is structured as follows: Section “**Methods**” delineates the methodological framework of trP-LCA, explaining how it tracks inventory changes while incorporating future scenarios. Section 3 presents and discusses the results, analyzing how different design strategies perform across future scenarios and temporal periods. Finally, Sect. 4 concludes with findings, and implications for sustainable building practices.

## 2 Methods

Our method expands upon the ISO 14040/14044 LCA framework (ISO: 14040 2006a; ISO: 14044 2006b) by incorporating recovery potential assessment and temporal evolution. Before introducing our key methodological advances, we outline the foundational components established in Abu-Ghaida et al. (2024), indicated by gray sections in Fig. 2. These components form the essential groundwork for the enhanced approach presented in this paper.

The framework begins with Goal and Scope Definition (Sect. 1 of Fig. 2), establishing the system boundaries, functional unit, and assessment objectives. This foundational step directs all subsequent analyses and connects directly to the DfD Assessment (Sect. 3). Supporting Data (Sect. 2) encompasses four critical data categories: LCI databases, EoL scenarios, Transport scenarios, and Service Life scenarios.

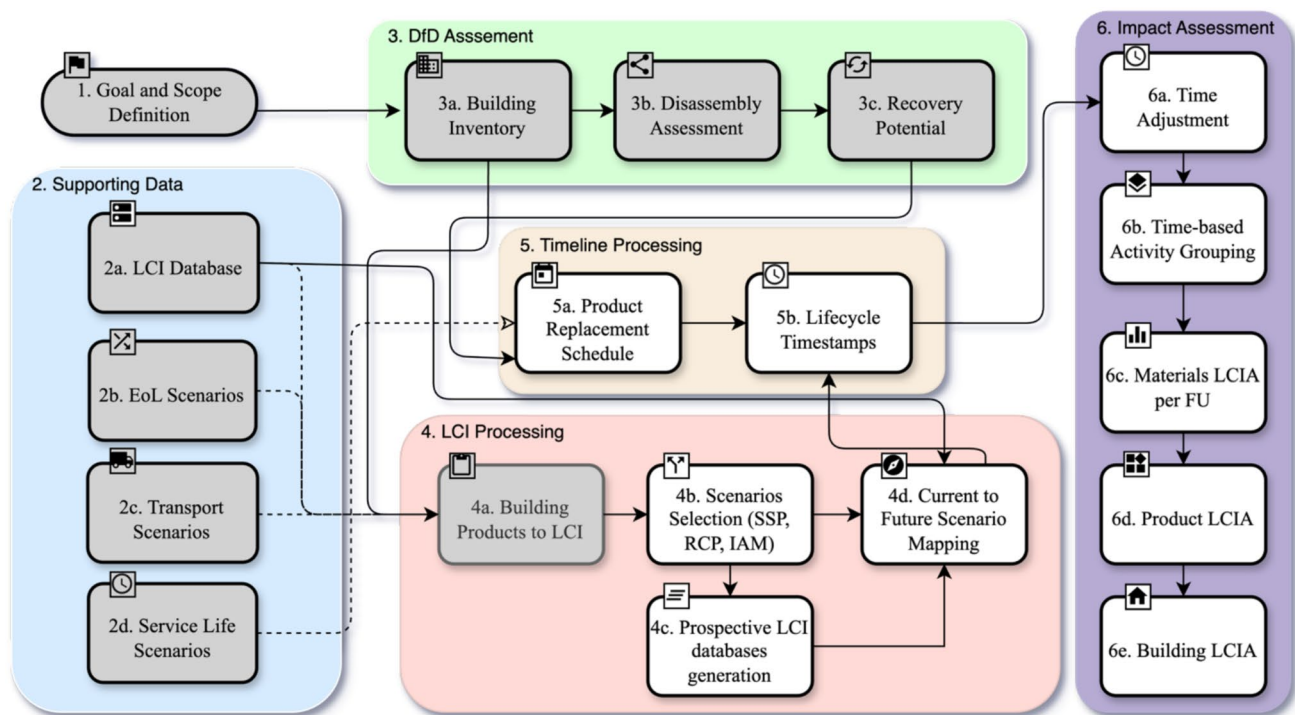


**Fig. 2** Overview of computational structure for performing trP-LCA. Gray sections represent the established methodology from Abu-Ghaida et al. (2024), white sections show additions made to establish the trP-LCA

The DfD Assessment (Sect. 3) quantifies recovery potential through a systematic process that first creates a detailed Building Inventory (Sect. 3a) cataloging all construction materials and components. This inventory feeds into the Disassembly Assessment (Sect. 3b), which evaluates the ease of building disassembly using indicators such as connection types, accessibility, form containment, and crossings. The assessment culminates in calculating Recovery Potential (Sect. 3c), determining the likelihood of successfully recovering components for reuse or repurposing.

The paper builds upon this foundation by introducing temporal dynamics and scenario-based projections, represented by the white sections in Fig. 2. These enhancements capture how technological advancement, energy system evolution, and policy changes affect the environmental burden of producing, transporting, and disposing of materials throughout a building's lifetime.

To fulfill these assessment objectives, the methodology is applied to a specific building case study where we analyze three distinct configurations to evaluate the environmental benefits of DfD principles. The first is a BAU scenario, which represents a zero-energy building as constructed with limited DfD practices. The second is a HDP scenario that maximizes connection reversibility by optimizing all connections to achieve the highest possible disassembly potential score of 1.0; this involved assuming reversible

mechanical fasteners replaced adhesives or destructive connections. The third is a LDP scenario representing a theoretical worst-case, where easily accessible connections were assumed to be replaced with embedded or destructive types, assigned the lowest possible score of 0.1.

The methodological framework, case study, and these design variants build directly upon our previous work (Abu-Ghaida et al. 2024). In that foundational study, we explored the impact of different service life and recovery potential assumptions. The primary goal of this current research is to extend that static framework into a time-resolved prospective one to assess how DfD benefits perform under evolving future conditions.

To isolate the impact of the newly introduced temporal dynamics, namely, the projected changes in background LCI data, we deliberately standardized other key parameters using the default median scenarios from our previous analysis. The building's service life is set to a median value of 60 years. For individual components, we utilize their median service lives based on statistical data from Goulouti et al. (2021) following the methodology established in our prior work (Abu-Ghaida et al. 2024). The relationship between disassembly potential (DP) and recovery potential (RP) is modeled using the default S-curve (S1). Furthermore, the analysis was updated from Ecoinvent v3.8 to v3.9.1 to ensure the use of the most current background data for our baseline. By



holding these parameters constant, we can confidently attribute the observed differences in environmental performance to the temporal evolution of background systems.

The inventory analysis phase employs three quantitative data sources: Building Information Modeling (BIM) models, technical drawings, and bills of materials. We structure this data hierarchically across five levels: material, product, assembly, system, and building, following the Level(s) framework (Dodd et al. 2017). Each product's data includes physical properties (mass, dimensions), functional roles, and specific disassembly sequences derived from reversing documented assembly steps. The inventory maps to LCI datasets from Ecoinvent 3.9.1 (Ecoinvent 2022) for production impacts, the Environmental profile of building elements (MMG) methodology (TOTEM 2021) for transport scenarios with defined distances and vehicle types, and Product Environmental Footprint (PEF) documentation for EoL pathways (European Commission 2019).

The disassembly network assessment employs Python-based directed network graphs to represent product interdependencies. Each edge represents a structural dependency (physical connection) or accessibility dependency (spatial relationship). We quantify four specific indicators for structural dependencies using fuzzy number logic: connection type (scored 0.1 – 1.0), connection access, form containment, and crossings (Durmisevic 2006).

Product disassembly potential calculation aggregates these scores using a weighted average approach, distinguishing between base products (structural components) and auxiliary products. This differentiation recognizes that auxiliary product removal should not impact base product disassembly potential. The resulting score ranges from 0.1 to 1.0, quantifying disassembly feasibility.

Recovery potential assessment builds on these scores using non-linear least squares regression with the Levenberg – Marquardt algorithm (Moré 1978), enabling systematic evaluation of various scenarios from linear to S-curve relationships between disassembly and recovery potential.

This paper extends this framework by introducing several key additions, as shown in Fig. 2. The Scenarios Selection (Sect. 4b) incorporates SSPs, RCPs, and IAMs to model potential future conditions, creating a foundation for time-resolved projections. The Prospective LCI Databases Generation (Sect. 4c) modifies baseline LCI data to reflect chosen future scenarios, accounting for evolving technologies, energy systems, and waste management practices. Current to Future Scenario Mapping (Sect. 4d) creates a correspondence between original Ecoinvent LCI datasets and their projected future versions, establishing a translation system that connects present-day inventory data with its projected future equivalents.

The Timeline Processing (Sect. 5) addresses the temporal aspects of the life cycle, determining when replacement

events occur (Sect. 5a) and assigning specific timestamps to all lifecycle events (Sect. 5b). Our previous methodology primarily determined replacement frequency to calculate total material flows. In contrast, this enhanced framework requires high resolution temporal positioning for each activity to apply the appropriate year-specific LCI data. In static LCA approaches, the actual timestamp of an activity is irrelevant since impacts are calculated using the same background data regardless of when the activity occurs. However, in trP-LCA, each lifecycle event must be evaluated using projected production, transport, and waste management technologies specific to its occurrence year, making temporal positioning critical for accurate impact assessment. The final Impact Assessment stage (Sect. 6) calculates environmental impacts by incorporating time adjustments (Sect. 6a), grouping activities by time for computational efficiency (Sect. 6b), and estimating impacts at material (Sect. 6c), product (Sect. 6d), and building (Sect. 6e) levels.

This approach represents the first integration of trP-LCA with recovery potential assessment for buildings. We project material and process impacts into the future (2015 – 2100), covering our case study building's construction in 2018 and the entire projection period available from current IAMs. Using IAMs, we achieve a higher temporal resolution than previous building LCAs through annual interpolation. Our method quantifies how embodied emissions differ from traditional static LCA results across nine distinct SSPs, IAMs, and RCP combinations.

The following sections detail how we transform this static recovery assessment into a trP-LCA framework for evaluating building design choices under various future pathways.

## 2.1 Life cycle inventory projection and temporal mapping

Buildings present unique challenges for life cycle assessment due to their extended lifespans. Our case study building, constructed in 2018 with an expected service life of 60 years, will remain operational until 2078. During this period, building components will require multiple replacements, each occurring under potentially different future conditions. For example, a window installed in 2018 might need replacement in 2048, when production technologies, energy systems, and recycling capabilities will likely differ from present conditions. This temporal complexity necessitates projecting environmental impacts from 2015 (the baseline year for our models) through 2100, ensuring coverage of the entire building lifecycle, including potential service life extensions up to 85 years.

To project these impacts, our framework uses scenarios built on the standard climate research matrix, which combines SSPs and RCPs. SSPs are narrative-based projections that describe plausible future societal developments,

outlining different global trajectories for demographics, economic growth, and policy implementation (O'Neill et al. 2014). They range from sustainable futures with low challenges for mitigation and adaptation (e.g., SSP1 “Sustainability”) to resource-intensive, fossil-fuel-dependent ones with high challenges (e.g., SSP5 “Fossil-fueled Development”) (O'Neill et al. 2014; Liao et al. 2023). In contrast, RCPs are not socioeconomic narratives but rather targets for climate outcomes, defined by the level of radiative forcing (the net change in the Earth’s energy balance) by the year 2100 (van Vuuren et al. 2011). These pathways represent different trajectories of GHG concentrations, corresponding to specific warming targets such as 1.5 °C or 2 °C (Lechtenberg et al. 2024). By combining an SSP with an RCP, a complete and consistent scenario is created, linking a societal pathway to a specific climate future, which is then modeled within an IAM (Cucurachi et al. 2022; Sacchi et al. 2022).

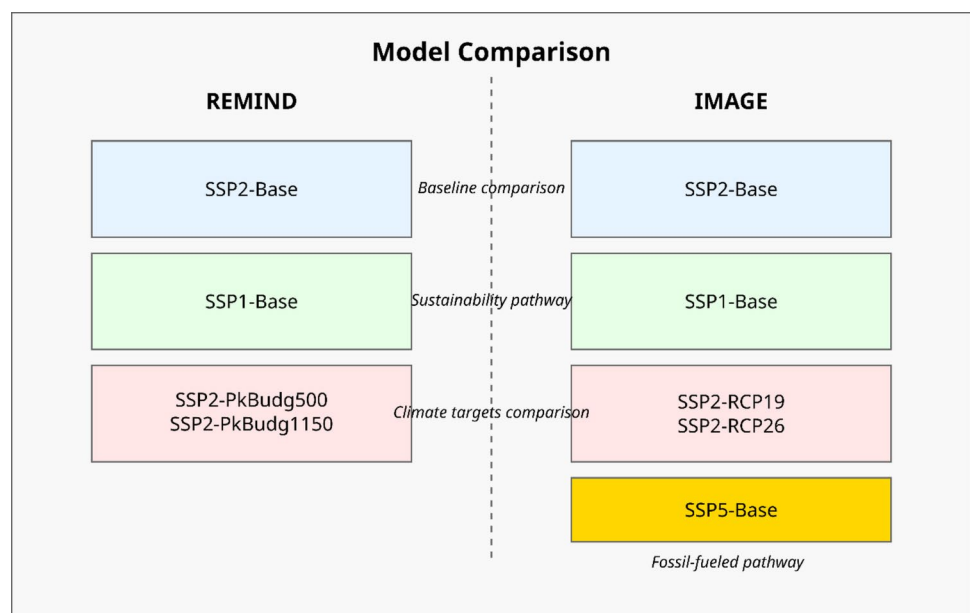
Following this framework, we implement nine selected scenarios to ensure consistent comparison across models while covering a range of potential future pathways, as shown in Fig. 3. The primary scenarios use SSP2 (“middle of the road” development), which represents moderate challenges for mitigation and adaptation, combined with three RCPs in each model. In REMIND, these scenarios are: SSP2-PkBudg500, aligned with RCP1.9 and aiming to limit warming to 1.5 °C with a 500 Gigatons (Gt) CO<sub>2</sub> budget from 2005 to 2100; SSP2-Base, which includes no additional climate policies beyond existing measures; and SSP2-PkBudg1150, aligned with RCP2.6 and pursuing a 2 °C target with an 1150 Gt CO<sub>2</sub> budget. IMAGE uses the equivalent combinations of SSP2 with RCP1.9, Base, and RCP2.6, respectively.

We supplement these primary scenarios with additional ones to explore a broader range of socioeconomic and climate futures. As shown in Fig. 3, we include SSP1 (“Sustainability”) Base scenarios from both models, representing a greener development pathway with lower challenges for mitigation and adaptation. We add an SSP5 (“Fossil-fueled Development”) Base scenario from IMAGE only, as REMIND does not model this high-emission pathway characterized by resource-intensive lifestyles and limited climate policy. By covering multiple SSPs and RCPs, our framework captures a spectrum of plausible socioeconomic trajectories and climate outcomes (O'Neill et al. 2014; van Vuuren et al. 2017).

For Prospective LCI database generation (Sect. 4c in Fig. 2), we utilize the PREMISE tool to generate projections based on the selected scenarios. PREMISE connects LCI databases with IAMs to create future-oriented inventories (Sacchi et al. 2022). We work with two complementary IAMs: IMAGE (Stehfest et al. 2014) and REMIND (Aboumahboub et al. 2020). IMAGE focuses on global environmental issues, land use, and natural resource management, employing a process-based approach to simulate interactions between human activities and ecosystems (Popp et al. 2014). REMIND centers on energy systems and climate mitigation strategies, utilizing an optimization framework to explore cost-effective energy-transition solutions (Gong et al. 2022). Together, these models provide comprehensive projections of how material production processes, energy systems, and waste management practices might evolve over time.

For each scenario, we create projections at five-year intervals from 2015 to 2100, yielding 18 timesteps. This temporal resolution matches the native output frequency of our IAMs while capturing significant technological transitions.

**Fig. 3** Selected scenario combinations across IMAGE and REMIND integrated assessment models



The process generates 162 distinct LCI databases (9 scenarios  $\times$  18 timesteps), each maintaining consistent system boundaries with Ecoinvent 3.9.1 while incorporating scenario-specific changes to energy carrier mixes, industrial process technologies, material production methods, transportation systems, and agricultural practices (Cox et al. 2020; Sacchi et al. 2022).

The final step in this section, Current to Future Scenario Mapping (Sect. 4d in Fig. 2), involves creating a correspondence between original Ecoinvent processes and their future projections across all scenarios and timesteps. The mapping process begins with Ecoinvent 3.9.1 as our baseline database, containing detailed quantification of current production processes, material flows, and environmental exchanges. For example, present-day steel production data includes specific energy requirements, material inputs, and emission factors. These values are then linked to their future equivalents in each projected database.

The mapping process requires significant data transformation to connect conventional LCI datasets with projected future equivalents. While PREMISE provides comprehensive projections, additional processing is needed to maintain data consistency across temporal boundaries and integrate with our building-specific inventory.

We store these mappings in a Structured Query Language (SQL) database optimized for efficient retrieval, with separate tables for activities, scenarios, impact categories, and calculation results. The implementation processes scenarios in batches of five timesteps to manage computational requirements while maintaining data consistency. Each batch generates complete projected databases before proceeding to the next, balancing processing efficiency with memory constraints.

## 2.2 Temporal framework for replacement activities

In this section, we explain how we establish time stamps for the entire life cycle of products and generate a product replacement schedule, as shown in Fig. 2 (Sect. 5a and 5b). Our approach extends the methodology detailed in Abu-Ghaida et al. (2024) by incorporating a time-resolved assessment. While our previous work already determined when replacements would occur to calculate their frequency, this enhanced framework requires precise temporal positioning of each activity to apply the appropriate year-specific LCI data.

The timeline establishment process involves two main steps: creating a primary replacement timeline and adjusting it based on interdependencies between products. First, we create a primary replacement timeline by comparing each product's service life with the building's lifetime. For instance, if a product has a lifetime of 20 years and the building's lifetime is 40 years, the product will need replacement

at year 20. This process is repeated for all products in the building system.

Next, we consider product interdependencies. For instance, even if product Y normally lasts 50 years, if it is a subcomponent of product X and cannot be separated, it must be replaced concurrently with X at year 20. This adjustment ensures that cascading effects are accurately captured.

We then make further adjustments to account for the cascading effects of replacements. Consider a scenario where product A lasts 10 years, and its child product B lasts 15 years but cannot be disassembled. When A is replaced at year 10, B must also be replaced. This shifts B's first replacement from its initially scheduled year 15 to year 10 (coinciding with A's replacement), subsequently shifting B's next replacement to year 25. These adjustments are made across all products to create a comprehensive replacement timeline.

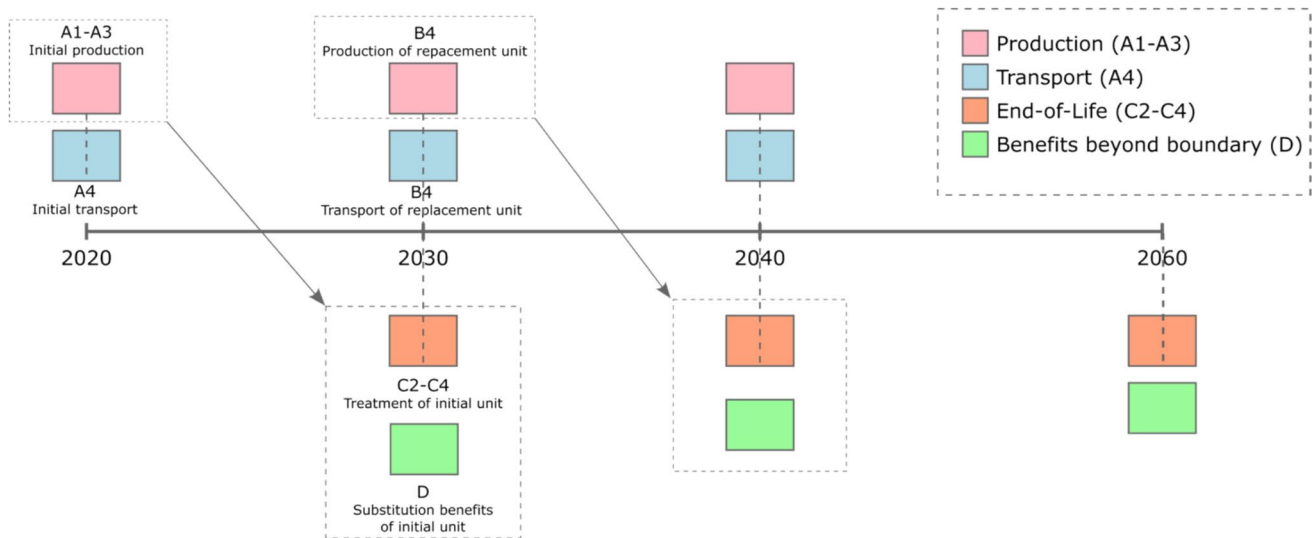
Unlike static prospective LCA approaches that apply current technology levels to all future activities, our time-resolved approach assigns temporally specific impact data to each activity based on when it occurs. This fundamentally changes how environmental impacts are calculated and allocated throughout the building's lifecycle, as illustrated in Fig. 4.

Figure 4 demonstrates how impacts are allocated along the building's lifetime. The timeline begins with mapping primary product replacements based on service life comparisons. Each replacement event triggers a cascade of activities, including production, transport, installation, and EoL treatment of the replaced components. Rather than using fixed impact factors as in our previous paper, each activity's environmental burden is calculated using data projected for its specific year of occurrence.

For example, when a product requires replacement in 2030, its production impacts are calculated using projected 2030 manufacturing technologies and energy systems rather than baseline data from 2018. This temporal specificity captures expected improvements in production efficiency, evolution of energy grids, and advancements in material processing between the building's construction and each replacement event. As shown in Fig. 4, each component's EoL impacts (orange boxes) occur after its replacement, creating a time lag between production and disposal impacts that cannot be captured in static assessments.

The approach becomes particularly significant when considering interdependent products. If product A's replacement in 2030 forces the replacement of product B due to accessibility constraints, B's replacement impacts are calculated using 2030 technology levels, even if B's intended service life extends beyond that point.

EoL treatment showcases another key difference between static and time-resolved approaches. Rather than applying current waste management capabilities to all future disposal



**Fig. 4** Temporal distribution of life cycle impacts showing how building components generate production, transport, EoL, and recovery benefit impacts at their specific occurrence years throughout the building's lifespan

activities, we project how treatment technologies and their associated impacts evolve over time. A product reaching EoL in 2050 has its disposal impacts calculated using projected 2050 waste management technologies and systems. Similarly, the benefits beyond the system boundary (green boxes in Fig. 4) are also calculated using the appropriate year-specific data.

The resulting timeline provides a year-by-year overview of material flows and their associated impacts, reflecting how technological advancement and system evolution affect environmental burdens over time. This time-resolved approach enables a higher temporal resolution assessment of long-lived systems like buildings, where assuming static technology levels throughout the lifecycle would distort actual environmental impacts (Levasseur et al. 2010; Miller et al., 2013).

### 2.3 Time-resolved impact assessment and multi-level aggregation

This section covers the final stages of our methodology as shown in Fig. 2: Time Adjustment (Sect. 6a), Time-based Activity Grouping (Sect. 6b), and the calculation of impacts at material, product, and building levels (Sects. 6c-6e).

The life cycle impact assessment (LCIA) at the product level uses 26 distinct impact categories, comprising the Environmental Footprint (EF) 3.1 method's standard 25 categories (European Commission 2019) plus the Intergovernmental Panel on Climate Change (IPCC) 2021 global warming potential methodology. This additional GWP metric incorporates biogenic CO<sub>2</sub> flows and accounts for net negative emission technologies, which is

particularly relevant for analyzing future scenarios where carbon capture technologies become more prevalent (Sacchi et al. 2022). The results section focuses primarily on GWP due to buildings' significant role in climate change mitigation strategies.

Following Fig. 2, we first implement time adjustment for LCI data (Sect. 6a). The IAMs provide data at 5-year intervals from 2015 to 2100, but our analysis requires annual resolution to match replacement timelines. We apply linear interpolation, a common approach when higher-resolution trend data is unavailable, between available timesteps (see Supplementary Information S1). This adjustment ensures that each activity is associated with temporally appropriate inventory data.

For computational efficiency, we implement Time-based Activity Grouping (Sect. 6b in Fig. 2). This process identifies instances where identical activities occur at the same timestamp across multiple building components. For example, if both steel beams and columns require "steel production" activity in 2018, we calculate this impact once with the combined quantity rather than processing it twice. This eliminates redundant calculations while maintaining assessment accuracy.

For Materials LCIA per Functional Unit (Sect. 6c), we calculate impacts for each material's entire lifecycle. Initial production impacts (Modules A1-A3) are calculated for the building's construction year (2018), incorporating material extraction, processing, and manufacturing based on quantities determined in the inventory analysis. Transport impacts (A4) are similarly computed for 2018 using standard average distances from the MMG methodology (TOTEM 2021).



The Product LCIA calculation (Sect. 6d) aggregates material-level impacts to product-level, accounting for replacement cycles identified in the Temporal Framework section. Each replacement generates two distinct temporal impacts: EoL treatment of the original product and production/transport of its replacement. Unlike static LCA approaches, each activity's environmental impact is calculated using the projected data specific to its occurrence year, capturing technological advancements and system changes over time.

EoL processes include transport to waste management facilities (C2), material sorting (C3), and final disposal (C4). Module D captures benefits beyond the system boundary, particularly environmental advantages from material recovery based on recovery potentials determined through disassembly network analysis.

For Building LCIA (Sect. 6e), we aggregate product-level results across all nine scenarios, creating a comprehensive assessment matrix that captures variations across IAMs (REMIND/IMAGE), RCPs (1.9, 2.6, Base, PkBudg500, PkBudg1150), and SSPs (1, 2, 5). Our database organization preserves temporal resolution by storing impacts with corresponding timestamps, enabling aggregated analysis and time-series visualization.

The assessment maintains consistency with the ISO 14040/14044 framework while extending it to incorporate time-resolved elements. For interpretation, we compare the three building configurations (BAU, HDP, LDP) across different future scenarios to evaluate how design choices perform under various potential futures. We maintain consistent system boundaries and functional units (per square meter of floor area over 60 years) across all comparisons to ensure valid evaluation of environmental performance differences.

### 3 Results and discussion

This section presents and analyzes the environmental performance of different building designs across multiple assessment methods and future scenarios, directly addressing our two primary research questions: (1) how trP-LCA estimates differ from static LCA for building embodied emissions, and (2) whether DfD environmental benefits persist across diverse future scenarios. Our analysis first quantifies these differences through a comprehensive comparison of assessment approaches and then examines the underlying drivers and temporal patterns that explain these results.

Our analysis evaluates three consistently defined building design variants: (1) BAU – our case study building with standard DfD implementation; (2) HDP – the same building with connections optimized to maximize disassembly potential ( $DP = 1.0$ ); and (3) LDP – the building with connections redesigned for minimal disassembly consideration

( $DP = 0.1$ ). By examining these designs across nine distinct future scenarios spanning sustainable development (SSP1), middle-of-the-road (SSP2), and fossil-fueled development (SSP5) pathways, as well as climate policies targeting different warming thresholds ( $1.5^{\circ}\text{C}$  and  $2^{\circ}\text{C}$ ), we provide robust evidence for the environmental benefits of enhanced disassembly potential under diverse future conditions.

While our method assessed 25 environmental impact categories according to the EF 3.1 methodology, we focus on global warming potential (GWP) measured in  $\text{kg CO}_2 \text{ eq/m}^2$ . This focus is justified by the building sector's significant role in climate change mitigation strategies and because IAMs like IMAGE primarily explore pathways to reach climate targets, with less reliable modeling of mechanisms important to other impact categories (Bruhn et al. 2023). Results for all impact categories are provided in Supplementary material S2, where similar patterns of relative performance between designs and assessment methods are generally observed.

#### 3.1 Comparative assessment of building designs: static versus trP-LCA

Our analysis reveals differences in environmental impact estimates between static LCA and trP-LCA approaches across all building designs. These differences highlight the importance of methodological choices when assessing long-lived infrastructure such as buildings.

Figure 5 illustrates the evolution of cumulative GHG emissions from 2018 to 2078 for the three building designs. To account for future uncertainty, each design is evaluated across the nine distinct future scenarios detailed in Sect. 2. The solid line for each design represents the arithmetic mean of the GHG emissions across these nine scenarios. The corresponding shaded area depicts the full range of outcomes (the variation zone), from the most optimistic (lowest emissions) to the most pessimistic (highest emissions) future pathway.

Analyzing the mean trajectory, the BAU design exhibits distinct increases around 2040, 2055, and again just before EoL in 2078, each corresponding to major replacement cycles when multiple large components (e.g., cladding, finishes) simultaneously reach the end of service. These spikes are amplified in the LDP design, where low disassembly potential forces the removal of otherwise functional materials. In contrast, the HDP design shows fewer and smaller spikes because individual elements can be replaced with minimal disruption to adjacent products, producing a smoother cumulative emissions trajectory.

By the building's mid-life (around 2048), HDP averages roughly  $483 \text{ kg CO}_2 \text{ eq/m}^2$ , compared to 527 for BAU and 556 for LDP. This gap underscores how higher disassembly potential dampens replacement-driven emissions. The dashed lines represent static LCA results, which remain

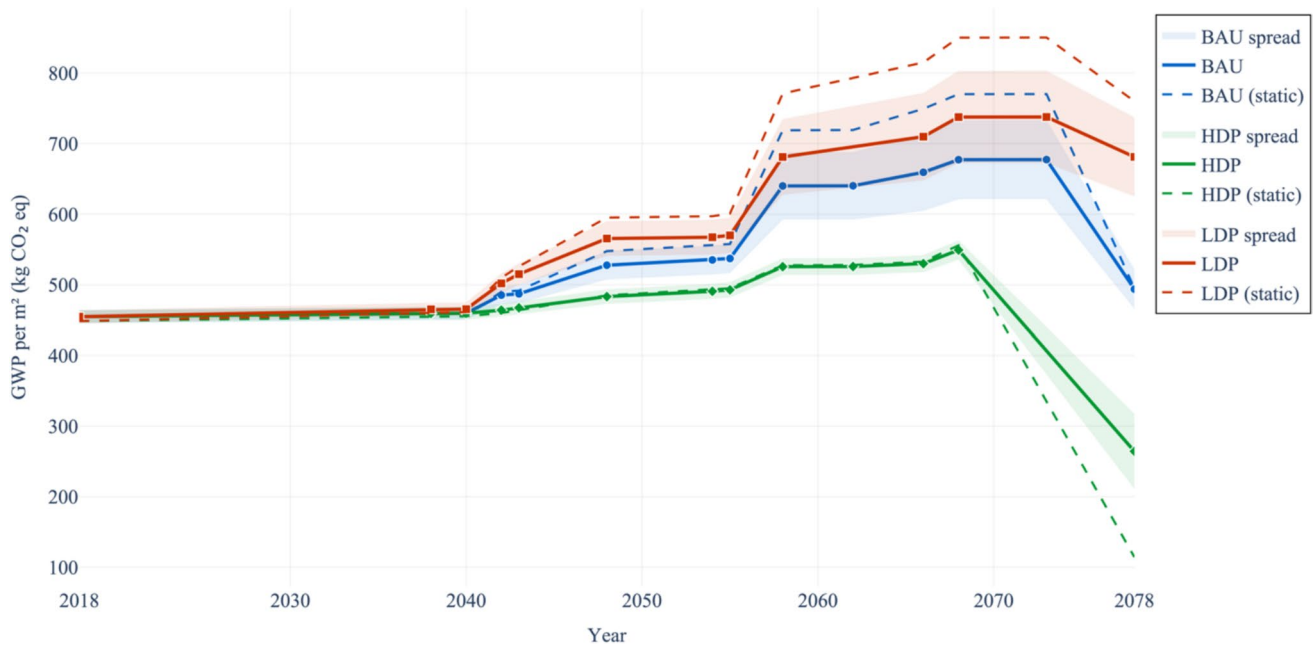


**Fig. 5** Cumulative GHG emissions across different building designs and scenarios over the 60-year service life. Solid lines represent the arithmetic mean across the nine future scenarios studied. Shaded areas indicate the full range of outcomes (min – max) across these

scenarios, reflecting the uncertainty from different socioeconomic and climate pathways. Markers indicate specific impact events, and dashed lines show static LCA results for comparison

above the average trP-LCA trajectories after about 2040. By 2078, static LCA can overestimate BAU's total embodied emissions by up to 32% in the most optimistic scenario. This discrepancy arises because static LCA cannot capture the gradual decarbonization of future production processes, especially during later replacements.

The slight downward turn at the end of the building's life (2078) is directly related to the application of end-of-life recovery credits from Module D. This decline in the cumulative curve occurs because the environmental benefit of recovering materials, which avoids the future production of new materials, is subtracted from the building's total lifetime emissions. This finding aligns with other prospective studies indicating that circular strategies, such as

reuse or recycling, offer fewer emission reductions when future manufacturing is significantly decarbonized.

Table 1 compares the GHG emission estimates derived from static LCA and trP-LCA for the BAU, HDP, and LDP designs with and without Module D benefits. Overall, static LCA tends to yield higher emissions for BAU compared to trP-LCA; for example, static LCA estimates BAU emissions at 828 kg CO<sub>2</sub> eq/m<sup>2</sup> (excluding Module D), whereas trP-LCA projects a range from 627 to 822 kg CO<sub>2</sub> eq/m<sup>2</sup>, an overestimation of up to 32%.

In contrast, the HDP design consistently exhibits lower emissions than BAU. Under static LCA, BAU registers 828 kg CO<sub>2</sub> eq/m<sup>2</sup> (excluding Module D) compared to 596 kg CO<sub>2</sub> eq/m<sup>2</sup> for HDP, a reduction of approximately

**Table 1** Comparison of GHG emissions (kg CO<sub>2</sub> eq/m<sup>2</sup>) between trP-LCA and Static-LCA methods across three building design variants, showing percentage differences with and without Module D benefits. Note: "Negative difference indicates trP-LCA results are lower than static LCA"

System boundary	Design	trP-LCA (min – max)	Static LCA	Difference (%)
Total excluding module D	BAU	(626.7) – (821.54)	828.42	(–32.19%) – (–0.84%)
	HDP	(549.81) – (614.22)	596.48	(–8.49%) – (2.89%)
	LDP	(683.03) – (909.48)	920.84	(–34.82%) – (–1.25%)
Total including module D	BAU	(441.87) – (532.21)	496.4	(–12.34%) – (6.73%)
	HDP	(180.48) – (336.29)	115.07	(36.24%) – (65.78%)
	LDP	(604.29) – (784.96)	764.75	(–26.55%) – (2.57%)

28%. When Module D benefits are included, static LCA estimates are 496 kg CO<sub>2</sub> eq/m<sup>2</sup> for BAU and 115 kg CO<sub>2</sub> eq/m<sup>2</sup> for HDP. This difference corresponds to a reduction of about 77% for HDP relative to BAU, demonstrating the environmental advantage of high disassembly potential. Conversely, the LDP design yields higher embodied emissions than BAU under all conditions. Under static LCA, LDP's emissions are about 11% greater than BAU (920 vs 828 kg CO<sub>2</sub>/m<sup>2</sup> excluding Module D), and when including Module D benefits the gap widens to ~54% (765 vs 496 kg CO<sub>2</sub>/m<sup>2</sup>). This consistent pattern across assessment methods confirms that poor disassembly potential worsens environmental performance regardless of methodological approach or future scenario.

These findings underscore that static LCA does not account for the gradual decarbonization of production processes over time. While static LCA applies current production impacts uniformly to all future activities, trP-LCA adjusts for anticipated technological improvements and cleaner production methods. As future manufacturing becomes less GHG-intensive, the benefits from avoided production, captured as Module D credits, diminish accordingly. This pattern is consistent with the results reported by Šimaitis et al. 2023 on lithium-ion batteries, which found that recycling benefits could decrease by up to 75% in future scenarios with decarbonized electricity, potentially leading to higher net impacts (Šimaitis et al. 2023). This outcome underscores why temporal specificity is essential for evaluating circular economy strategies, which derive much of their environmental benefit from avoiding future production (Gallego-Schmid et al. 2020).

The implications for decision-making in the building sector are clear: failing to incorporate temporal dynamics can lead to suboptimal design choices, particularly for long-lived structures with multiple replacement cycles. A

more detailed stage-by-stage analysis is essential to identify the key drivers behind these aggregate differences and to inform targeted strategies for sustainable building design.

To understand the drivers behind the overall differences in environmental performance, we further disaggregated GHG emissions by life cycle stage (see Table 1). This analysis reveals that the most considerable divergences between static LCA and trP-LCA occur during the replacement phase (B4) and in Module D benefits. At the same time, production (A1 – A3) and transport (A4) stages show minimal variation.

Table 2 presents the breakdown of GHG emissions by life cycle stage for each building design, comparing static LCA with trP-LCA results. Both methods yield nearly identical values for production, approximately 445 kg CO<sub>2</sub> eq/m<sup>2</sup>, which is expected since initial production occurs in 2018, close to the baseline year. Similarly, transport impacts are similar across all designs, with only minor differences between methods.

In contrast, the replacement phase shows larger differences. For BAU, static LCA estimates replacement emissions at about 337 kg CO<sub>2</sub> eq/m<sup>2</sup>, while trP-LCA projections range from roughly 147 to 307 kg CO<sub>2</sub> eq/m<sup>2</sup>. This suggests that static LCA can overestimate replacement emissions by as much as 130% in more sustainable scenarios due to its inability to account for the gradual decarbonization of production processes over time. Notably, the HDP design exhibits much lower replacement emissions; static LCA indicates about 122 kg CO<sub>2</sub> eq/m<sup>2</sup> for HDP, nearly 64% lower than BAU, while trP-LCA shows a similar trend across scenarios. Conversely, the LDP design incurs a higher replacement burden compared to BAU, confirming that poor disassembly potential exacerbates environmental impacts during component replacement.

**Table 2** Breakdown of greenhouse gas emissions (kg CO<sub>2</sub> eq/m<sup>2</sup>) by life cycle stage for each building design, comparing static LCA with trP-LCA ranges and highlighting percentage differences between methods across production (A1–A3), transport (A4), replacement (B4), EoL (C), and benefits (D) phases

System boundary	Design	Static LCA	trP-LCA (min – max)	Difference (%)
A1–A3	BAU	444.59	(441.01) – (465.37)	(–0.81%) – (4.47%)
	HDP	444.59	(441.01) – (465.37)	(–0.81%) – (4.47%)
	LDP	444.59	(441.01) – (465.37)	(–0.81%) – (4.47%)
A4	BAU	3.79	(3.64) – (3.78)	(–4.12%) – (–0.26%)
	HDP	3.79	(3.64) – (3.78)	(–4.12%) – (–0.26%)
	LDP	3.79	(3.64) – (3.78)	(–4.12%) – (–0.26%)
B4	BAU	336.83	(146.55) – (307.03)	(–129.84%) – (–9.71%)
	HDP	122.34	(77.21) – (117.58)	(–58.45%) – (–4.05%)
	LDP	414.38	(190.21) – (380.03)	(–117.85%) – (–9.04%)
C	BAU	43.21	(32.99) – (45.35)	(–30.98%) – (4.72%)
	HDP	25.75	(18.91) – (27.48)	(–36.17%) – (6.3%)
	LDP	58.07	(44.58) – (60.29)	(–30.26%) – (3.68%)
D	BAU	–332.02	(–289.33) – (–160.92)	(–14.75%) – (–106.33%)
	HDP	–481.41	(–409.47) – (–219.67)	(–17.57%) – (–119.15%)
	LDP	–156.08	(–144.38) – (–78.75)	(–8.1%) – (–98.2%)

EoL impacts (C) also differ between methods, with static LCA overestimating these impacts by up to 31% for BAU. Module D benefits reveal a critical insight: for BAU, static LCA applies a uniform credit of around  $-332 \text{ kg CO}_2 \text{ eq/m}^2$ , whereas trP-LCA yields a range from about  $-289$  to  $-161 \text{ kg CO}_2 \text{ eq/m}^2$ . This variation highlights that as production processes become cleaner in future scenarios, the environmental benefit of avoiding new production through material recovery diminishes.

This stage-by-stage analysis shows that replacement impacts, and Module D benefits are the primary contributors to the aggregate differences between static LCA and trP-LCA. These findings emphasize the importance of incorporating temporal dynamics into LCA, providing more targeted insights for sustainable building design and more accurate assessments of long-term environmental performance.

### 3.2 Influence of future development pathways on DfD benefits

We now examine how future development pathways influence the environmental benefits of DfD. Table 3 presents the three building designs' GHG emissions across socioeconomic scenarios (SSP1-Base, SSP2-Base, SSP5-Base). Under the middle-of-the-road SSP2-Base scenario, BAU produces intermediate emissions, while HDP consistently reduces emissions by about 25% relative to BAU. In contrast, LDP increases emissions by roughly 11% compared to BAU. Under the sustainable SSP1-Base scenario, BAU emissions are approximately 4% lower than under SSP2-Base, reflecting cleaner background technologies; however, HDP still achieves nearly a 24% reduction relative to BAU. In the fossil-fueled SSP5-Base scenario, overall emissions are highest, yet HDP maintains a reduction of around 25%

relative to BAU, and LDP remains about 11% higher. These trends indicate enhanced disassembly potential offers robust environmental benefits regardless of socioeconomic development trajectories.

Conversely, under the fossil-fueled SSP5-Base scenario modeled by REMIND, BAU emissions increase to  $822 \text{ kg CO}_2 \text{ eq/m}^2$ . In this less sustainable future, HDP still performs strongly, reducing emissions to approximately  $614 \text{ kg CO}_2 \text{ eq/m}^2$ , a reduction of about 25% relative to BAU. LDP again exhibits higher emissions, reaching roughly  $909 \text{ kg CO}_2 \text{ eq/m}^2$ , or 11% above BAU. These consistent trends across SSPs illustrate that the benefits of DfD are robust regardless of socioeconomic development trajectories.

Table 4 extends the analysis to climate policy scenarios. Under the IMAGE-RCP1.9 scenario (targeting  $1.5^\circ \text{C}$  warming), BAU emissions are reduced to  $627 \text{ kg CO}_2 \text{ eq/m}^2$ , reflecting the impact of aggressive decarbonization measures. In this context, HDP achieves emissions of  $550 \text{ kg CO}_2 \text{ eq/m}^2$ , a reduction of about 12% compared to BAU. Although the absolute differences are minor in a highly constrained climate scenario, the ranking of designs remains consistent.

Under IMAGE-RCP2.6 (aligned with a  $2^\circ \text{C}$  target), BAU emissions increase slightly to  $654 \text{ kg CO}_2 \text{ eq/m}^2$ , while HDP registers around  $561 \text{ kg CO}_2 \text{ eq/m}^2$ . The relative reduction in this case is approximately 14%. These results indicate that the relative advantage of enhanced disassembly potential can increase as climate policies become less stringent.

The REMIND peak budget scenarios further reveal nuanced differences. In the PkBudg500 scenario (aligned with a  $1.5^\circ \text{C}$  target), BAU emissions are estimated at  $653 \text{ kg CO}_2 \text{ eq/m}^2$ , with HDP reducing emissions to about  $556 \text{ kg CO}_2 \text{ eq/m}^2$ , a 15% reduction. In the less restrictive

**Table 3** GHG emissions ( $\text{kg CO}_2 \text{ eq/m}^2$ ) across socioeconomic pathways for all building designs, with percentage changes from BAU shown in parentheses

Design	SSP1-Base (IMAGE)	SSP2-Base (IMAGE)	SSP5-Base (REMIND)
BAU	751.52	783.17	821.54
LDP	826.85 (+10.0%)	866.85 (+10.7%)	909.48 (+10.7%)
HDP	574.16 (−23.6%)	584.72 (−25.3%)	614.22 (−25.2%)

In the sustainable SSP1-Base scenario, BAU emissions decline to  $752 \text{ kg CO}_2 \text{ eq/m}^2$ , approximately 4% lower than under SSP2-Base. Despite the overall cleaner background conditions, the HDP design still substantially reduces emissions, with levels around  $574 \text{ kg CO}_2 \text{ eq/m}^2$ . This represents nearly a 24% improvement over BAU. Even though absolute emissions are lower in a sustainable development context, the relative advantage of enhanced disassembly potential remains pronounced

**Table 4** GHG emissions ( $\text{kg CO}_2 \text{ eq/m}^2$ ) across climate policy scenarios with percentage changes from BAU shown in parentheses

Design	RCP1.9 (IMAGE)	RCP2.6 (IMAGE)	pkBudg500 (REMIND)	pkBudg1150 (REMIND)
BAU	626.7	653.58	652.87	680.9
LDP	683.03 (+9.0%)	718.31 (+9.9%)	705.39 (+8.0%)	737.98 (+8.4%)
HDP	549.81 (−12.3%)	561.07 (−14.2%)	555.96 (−14.8%)	565.02 (−17.0%)



PkBudg1150 scenario (aligned with a 2 °C target), BAU emissions climb to 681 kg CO<sub>2</sub> eq/m<sup>2</sup>, and HDP achieves emissions of roughly 565 kg CO<sub>2</sub> eq/m<sup>2</sup>, corresponding to a 17% reduction relative to BAU.

These climate policy scenarios indicate that aggressive decarbonization measures lead to lower absolute emissions for all designs, narrowing the gap between them. However, the consistent relative ranking, with HDP outperforming BAU and BAU outperforming LDP, demonstrates that enhanced disassembly potential offers environmental benefits under any climate policy scenario. In contrast, LDP consistently increases emissions by about 8 – 10% relative to BAU, regardless of the policy pathway.

The variation in absolute benefits across scenarios has important implications for policy development. In scenarios with strict climate targets (such as RCP1.9), the overall emission reductions are smaller because all designs benefit from cleaner production processes. For instance, under IMAGE-RCP1.9, HDP reduces emissions by approximately 77 kg CO<sub>2</sub> eq/m<sup>2</sup> compared to BAU, whereas under SSP2-Base, the reduction is nearly 198 kg CO<sub>2</sub> eq/m<sup>2</sup>. This suggests that while DfD remains beneficial in all cases, its absolute impact depends on the broader decarbonization context.

When both socioeconomic and climate policy scenarios are considered together, the absolute emissions of all designs decline in scenarios with greater technological improvements and stricter climate policies. However, the relative performance, HDP performing best, followed by BAU and LDP, remains stable. This stability provides strong guidance for building designers and policymakers, confirming that enhanced disassembly potential is a robust strategy for reducing embodied emissions.

Despite differences in these two IAMs (IMAGE vs. REMIND), both yielded very similar relative performances for BAU, HDP, and LDP. This consistency across models reinforces confidence in our conclusion that enhanced disassembly potential offers environmental benefits under a range of future assumptions.

### 3.3 Hotspot analysis

The temporal distribution of environmental impacts across Brand's "shearing layers" (Brand 1995; Schmidt Iii And Austin 2016) provides insight into how each building system contributes to overall GHG emissions over time. Figure 6 illustrates these accumulations for Structure, Skin, Space Plan, and Services, comparing static LCA (dashed lines) with time-resolved results (solid lines). HDP emits less than BAU in each layer, while LDP shows higher emissions. The shaded bands reflect uncertainty across scenarios, demonstrating that enhanced disassembly potential consistently lowers emissions regardless of future development pathways.

In the Structure panel (upper-left), structural elements dominate total embodied impacts, ranging from roughly 300 to 600 kg CO<sub>2</sub> eq/m<sup>2</sup>. While many structural components, such as columns or load-bearing walls, often remain for the building's full lifespan, some elements (e.g., floor slabs) can require partial replacement if embedded systems like under-floor heating must be accessed or upgraded. This nuance explains why structural layers may not remain entirely untouched in specific design variants. Figure 6 also shows static LCA consistently overestimating structural impacts beyond 2040, owing to its assumption of constant emission intensities for steel and concrete. By contrast, time-resolved projections incorporate future decarbonization, resulting in lower cumulative impacts.

The Skin panel (upper-right) indicates moderate replacement cycles around 2040 – 2050, increasing GWP from approximately 50 to 80 kg CO<sub>2</sub> eq/m<sup>2</sup>. All three design variants follow similar trajectories, suggesting that facade connections are less influenced by disassembly potential than structural or interior elements. The shaded bands are relatively narrow, indicating that changes in future background processes have a more negligible effect on Skin-related emissions than on more material-intensive systems like Structure.

The differences between designs are more pronounced in the Space Plan panel (lower-left). Emissions range from around 40 to 120 kg CO<sub>2</sub> eq/m<sup>2</sup>, with LDP reaching roughly 85 – 90 kg by 2060 versus about 55 – 60 kg for HDP. Notably, the BAU line appears nearly identical to HDP in this layer, so it overlaps visually. The steeper steps in the LDP design highlight how interdependent interior components drive cascading replacements when the disassembly potential is low. In contrast, HDP's gradual increases indicate selective replacement without disturbing adjacent materials.

The Services panel (lower-right) has the lowest absolute GWP but exhibits distinct replacement cycles every 15 – 20 years, causing sharp emission spikes, especially in the LDP design. By 2060, LDP can reach around 55 – 60 kg CO<sub>2</sub> eq/m<sup>2</sup>, whereas HDP remains closer to 30 – 35 kg. Once again, static LCA overestimates these service-layer impacts as the building ages, diverging from time-resolved results that account for cleaner future manufacturing processes.

When comparing all layers, the figure confirms that static LCA (dashed lines) remains above time-resolved trajectories (solid lines), particularly after mid-life replacements. The Structure layer contributes the largest share of total emissions, followed by Space Plan, Skin, and Services. Across all panels, HDP yields consistently lower cumulative impacts than BAU, emitting less than LDP. These trends reinforce earlier findings that enhanced disassembly potential mitigates secondary replacements and enables greater recovery at end-of-life. The slight downward turn at 2078 in each

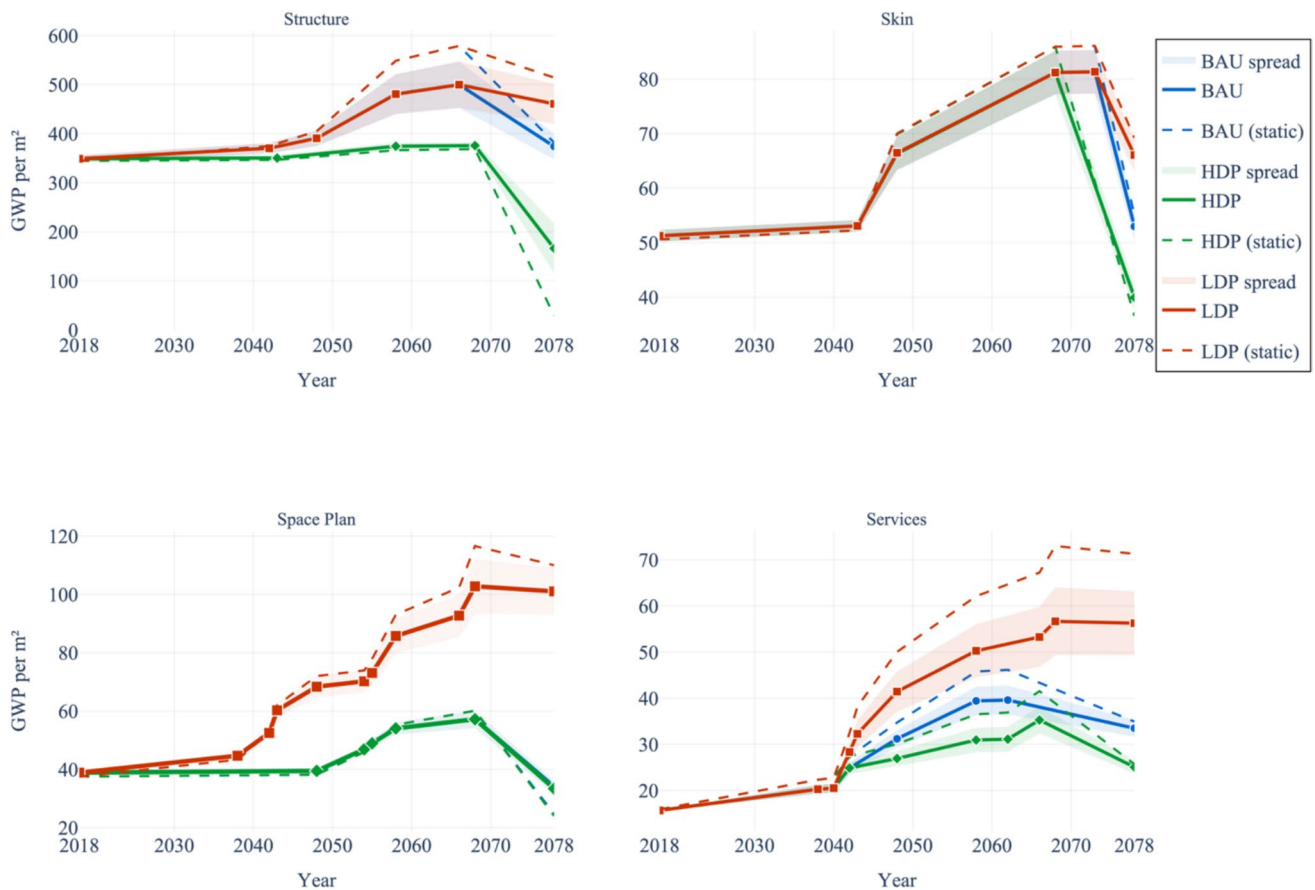


**Fig. 6** Cumulative GHG emissions across the Brand's shearing layers for different building designs over time. Static LCA results (dashed lines) consistently exceed trP-LCA results (solid lines), with shaded

areas representing scenario uncertainty ranges. HDP designs show lower emissions across all layers, with Space Plan and Services layers demonstrating the most relative improvements

panel reflects end-of-life recovery, with HDP consistently showing the steepest drop, indicating that it maximizes salvageable materials. Figure 6 demonstrates that while the absolute magnitude of emissions varies by layer, the relative ranking of design variants remains robust, highlighting DfD as an effective strategy in any future scenario.

These findings also carry significant policy implications by illuminating the relationship between two distinct mitigation approaches: system-level strategies that decarbonize the background supply chain and project-level strategies that focus on building design. Our analysis demonstrates that while system-level decarbonization (reflected in the cleaner SSP/RCP scenarios) reduces the absolute GHG benefits of DfD, the relative advantage of a high-disassembly design remains robust across all futures. This insight is crucial for policymakers, as it confirms that waiting for a fully decarbonized supply chain before mandating circular design principles would be a missed opportunity. The benefits of avoiding material replacements and enabling component reuse are consistently significant, regardless of how “clean” future production becomes. By quantifying the distinct

impacts of both approaches, the trP-LCA framework can help policymakers make more evidence-based decisions on resource allocation, comparing the environmental return on investment from different policies such as a subsidy for DfD-compliant connections versus R&D funding for green cement. Moreover, our results provide guidance on the timing of interventions, suggesting that project-level policies such as updating building codes to require DfD should be pursued in parallel with, not sequentially after, broader system-level decarbonization efforts, which often have longer implementation timelines. Future research could expand on this by incorporating a wider range of building typologies and regional contexts, thereby creating a more comprehensive decision-support tool for prioritizing investments that maximize long-term environmental benefits for the built environment.

### 3.4 Future research and limitations

This study has several limitations that warrant further investigation, beginning with the assumptions made to define its

scope. To clearly isolate the effect of transitioning from a static to a time-resolved prospective framework, we deliberately standardized several key parameters. For instance, while our previous work (Abu-Ghaida et al. 2024) investigated the significant impact of variations in building and component service life, we used fixed median service lives in this analysis. Other factors such as the specific building typology, regional context, and the potential impacts of climate change on material degradation were also held constant.

While these scoping choices allowed us to attribute our findings to the trP-LCA method, the framework itself presents areas for further development. First, the disassembly assessment method introduces additional uncertainties, particularly in quantifying the relationship between disassembly potential and material recovery; empirical validation is needed through actual building deconstruction projects. Second, the IAM projections, based on 5-year interpolations, simplify the complexity of technological transitions, and future studies should refine these projections for greater accuracy. Finally, our analysis focused primarily on GWP; while similar trends were observed in other impact categories, a more comprehensive sustainability assessment would include economic and social dimensions.

Future research should aim to validate the disassembly-recovery relationship through case studies and develop material passports that incorporate detailed disassembly parameters. Integration with Building Information Modeling and the expansion of the framework to include remanufacturability and refurbishability, as outlined in ISO 20887 (ISO: 20887 2020), would further enhance its applicability and accuracy in assessing the full sustainability potential of building designs.

## 4 Conclusion

This research advances building LCA methodology by transitioning from a static approach to trP-LCA, a dynamic framework incorporating projected changes in background LCI data. While this study focused specifically on assessing the environmental benefits of DfD our findings highlight the critical importance of this temporal approach for evaluating a wide range of circular economy strategies. The significant influence of future replacement cycles and evolving end-of-life credits, as demonstrated in our results, is not unique to DfD. Indeed, these dynamics are central to quantifying the benefits of durability, where the value of avoiding a future component replacement is directly tied to the decarbonization trajectory of manufacturing. Similarly, the trP-LCA method is essential for accurately assessing adaptability and flexibility, as the environmental savings from reconfiguring a space rather than demolishing it are

realized decades into the future. By demonstrating how to model these time-resolved impacts for DfD, this work provides a foundational template and a proof-of-concept for the prospective assessment of all long-term circular strategies in the built environment, ultimately supporting more robust and forward-looking design and policy decisions.

Our findings demonstrate that the environmental benefits of enhanced disassembly potential remain substantial across all future scenarios. Across sustainable development (SSP1) to fossil-fueled growth (SSP5) pathways, the HDP design consistently reduces embodied GHG emissions by 12 – 25% compared to BAU when excluding Module D benefits. In contrast, the LDP design exhibits higher emissions. These results indicate that the benefits of DfD derive primarily from reducing replacement requirements and enabling greater material recovery, mechanisms that remain effective regardless of future technological trajectories.

Transitioning from static LCA to trP-LCA alters absolute emission estimates while preserving the relative performance ranking among designs. Static LCA overestimates cumulative embodied GHG emissions by up to 32% relative to the most optimistic trP-LCA scenarios, particularly for replacement components produced decades after construction. Furthermore, our analysis reveals that the environmental credits for avoided production through material recovery decrease in scenarios with greater decarbonization. This confirms that temporal specificity is essential for accurately assessing long-lived systems with multiple replacement cycles.

This study confirms that enhanced disassembly potential is a robust strategy for reducing embodied emissions across various future pathways. Our work contributes to sustainable building design by providing a more dynamic LCA method that accounts for technological improvements over time. This new knowledge benefits building designers, policymakers, and environmental stakeholders by informing low-carbon construction strategies and supporting the transition to a circular economy, ultimately contributing to global sustainability efforts.

**Supplementary Information** The online version contains supplementary material available at <https://doi.org/10.1007/s11367-025-02526-8>.

**Acknowledgements** We would like to express our immense gratitude to InfraVitaal for providing us with the case study building. We also thank our colleagues from the Unit Water and Energy Transition at VITO for their valuable feedback on the methodology. Special appreciation goes to Chris Mutel and Romain Sacchi for answering questions and helping to solve coding-related issues during the development phase of this research.

**Author contribution** Conceptualization: H.A., S.L.; Methodology: H.A., S.L.; Software: H.A.; Validation: A.W.; Formal Analysis: H.A.; Data Curation: H.A., S.L.; Writing – Original Draft: H.A.; Writing – Review & Editing: H.A., A.H., M.R., A.W., S.L.; Visualization: H.A.;

Supervision: A.H., M.R., S.L.; Project Administration: S.L.; Funding Acquisition: S.L.

**Funding** This project has received funding from the European Union's Horizon 2020 research and innovation program under the Marie Skłodowska-Curie grant agreement No 956696.

**Data availability** The datasets generated during the current study are available in the Supplementary Information.

## Declarations

**Competing interests** The authors declare no competing interests.

**Open Access** This article is licensed under a Creative Commons Attribution-NonCommercial-NoDerivatives 4.0 International License, which permits any non-commercial use, sharing, distribution and reproduction in any medium or format, as long as you give appropriate credit to the original author(s) and the source, provide a link to the Creative Commons licence, and indicate if you modified the licensed material. You do not have permission under this licence to share adapted material derived from this article or parts of it. The images or other third party material in this article are included in the article's Creative Commons licence, unless indicated otherwise in a credit line to the material. If material is not included in the article's Creative Commons licence and your intended use is not permitted by statutory regulation or exceeds the permitted use, you will need to obtain permission directly from the copyright holder. To view a copy of this licence, visit <http://creativecommons.org/licenses/by-nc-nd/4.0/>.

## References

- Aboumahboub T, Auer C, Bauer N, Baumstark L, Bertram C, Bi S, Dietrich J, Dirnaichner A, Giannousakis A, Haller M, Hilaire J, Klein D, Koch J, Körner A, Kriegler E, Leimbach M, Levesque A, Lorenz A, Luderer G, Ludig S, Lüken M, Malik A, Manger S, Merfort L, Mouratiadou I, Pehl M, Pietzker R, Piontek F, Popin L, Rauner S, Rodrigues R, Roming N, Rottoli M, Schmidt E, Schreyer F, Schultes A, Sörgel B, Streffler J, Ueckerdt F (2020) REMIND - REgional Model of INvestments and Development - Version 2.1.0
- Abu-Ghaida H, Ritzen M, Hollberg A, Theissen S, Attia S, Lizin S (2024) Accounting for product recovery potential in building life cycle assessments: a disassembly network-based approach. *Int J Life Cycle Assess*. <https://doi.org/10.1007/s11367-024-02324-8>
- Anand CK, Amor B (2017) Recent developments, future challenges and new research directions in LCA of buildings: a critical review. *Renew Sustain Energy Rev* 67:408 – 416. <https://doi.org/10.1016/j.rser.2016.09.058>
- Arvidsson R, Tillman A-M, Sandén BA, Janssen M, Nordelöf A, Kushnir D, Molander S (2018) Environmental assessment of emerging technologies: recommendations for prospective LCA. *J Ind Ecol* 22:1286 – 1294. <https://doi.org/10.1111/jiec.12690>
- Brand S (1995) How buildings learn: what happens after they're built. Penguin
- Bruhn S, Sacchi R, Cimpan C, Birkved M (2023) Ten questions concerning prospective LCA for decision support for the built environment. *Build Environ* 242:110535. <https://doi.org/10.1016/j.buildenv.2023.110535>
- Buyle M, Braet J, Audenaert A (2013) Life cycle assessment in the construction sector: a review. *Renew Sustain Energy Rev* 26:379 – 388. <https://doi.org/10.1016/j.rser.2013.05.001>
- European Commission (2019) Product environmental footprint (PEF) method. [https://eplca.jrc.ec.europa.eu/permalink/PEF\\_method.pdf](https://eplca.jrc.ec.europa.eu/permalink/PEF_method.pdf). Accessed 28 Apr 2023
- European Commission (2021) Renovation and decarbonisation of buildings. [https://ec.europa.eu/commission/presscorner/detail/en/IP\\_21\\_6683](https://ec.europa.eu/commission/presscorner/detail/en/IP_21_6683). Accessed 10 Jul 2023
- Cox B, Bauer C, Mendoza Beltran A, van Vuuren DP, Mutel CL (2020) Life cycle environmental and cost comparison of current and future passenger cars under different energy scenarios. *Appl Energy* 269:115021. <https://doi.org/10.1016/j.apenergy.2020.115021>
- Cucurachi S, van der Giesen C, Guinée J (2018) Ex-ante LCA of emerging technologies. *Procedia CIRP* 69:463 – 468. <https://doi.org/10.1016/j.procir.2017.11.005>
- Cucurachi S, Steubing B, Siebler F, Navarre N, Caldeira C, Sala S (2022) Prospective LCA methodology for novel and emerging technologies for BIO-based products. *Publ Off Eur Union Luxemb*. <https://doi.org/10.2760/167543>
- Dodd N, Cordella M, Traverso M, Donatello S (2017) Level (s) – a common EU framework of core sustainability indicators for office and residential buildings: Parts 1 and 2: Introduction to Level (s) and how it works (Beta v1. 0)
- Durmisevic E (2006) Transformable building structures: design for disassembly as a way to introduce sustainable engineering to building design & construction
- Ecoinvent (2022) ecoinvent Version 3.9.1. <https://support.ecoinvent.org/ecoinvent-version-3.9.1>. Accessed 14 Jan 2025
- Fnaiss A, Rezgui Y, Petri I, Beach T, Yeung J, Ghoroghi A, Kubicki S (2022) The application of life cycle assessment in buildings: challenges, and directions for future research. *Int J Life Cycle Assess* 27:627 – 654. <https://doi.org/10.1007/s11367-022-02058-5>
- Frischknecht R, Stucki M (2010) Scope-dependent modelling of electricity supply in life cycle assessments. *Int J Life Cycle Assess* 15:806 – 816. <https://doi.org/10.1007/s11367-010-0200-7>
- Gallego-Schmid A, Chen H-M, Sharmina M, Mendoza JMF (2020) Links between circular economy and climate change mitigation in the built environment. *J Clean Prod* 260:121115. <https://doi.org/10.1016/j.jclepro.2020.121115>
- Gong C, Ueckerdt F, Pietzcker R, Odenweller A, Schill W, Martín, Kittel, Luderer G (2022) Bidirectional coupling of a long-term integrated assessment model with an hourly power sector model. <https://doi.org/10.5194/egusphere-2022-885>
- Goulouti K, Favre D, Giorgi M, Padey P, Galimshina A, Habert G, Lasvaux S (2021) Dataset of service life data for 100 building elements and technical systems including their descriptive statistics and fitting to lognormal distribution. *Data Brief* 36:107062. <https://doi.org/10.1016/j.dib.2021.107062>
- International Energy Agency (2021) Net zero by 2050: a roadmap for the global energy sector. [https://iea.blob.core.windows.net/assets/deebef5d-0c34-4539-9d0c-10b13d840027/NetZeroBy2050-ARoadmapfortheGlobalEnergySector\\_CORR.pdf](https://iea.blob.core.windows.net/assets/deebef5d-0c34-4539-9d0c-10b13d840027/NetZeroBy2050-ARoadmapfortheGlobalEnergySector_CORR.pdf). Accessed 3 Mar 2023
- ISO: 14040 (2006a) International Organization of Standardization. Environmental management – life cycle assessment – principles and framework
- ISO: 14044 (2006b) International Organization of Standardization. Environmental management – life cycle assessment – requirements and guidelines
- ISO (2020) 20887: 2020 Sustainability in buildings and civil engineering works – design for disassembly and adaptability – principles, requirements and guidance
- Lechtenberg F, Istrate R, Tulus V, España A, Graells M, Guillén-Gosálbez G (2024) PULPO: a framework for efficient integration of life cycle inventory models into life cycle product optimization. *J Ind Ecol* 28:1449 – 1463. <https://doi.org/10.1111/jiec.13561>



- Levasseur A, Lesage P, Margni M, Deschênes L, Samson R (2010) Considering time in LCA: dynamic LCA and its application to global warming impact assessments. *Environ Sci Technol* 44:3169–3174. <https://doi.org/10.1021/es9030003>
- Liao J, Tang L, Shao G (2023) Coupling random forest, allometric scaling, and cellular automata to predict the evolution of LULC under various shared socioeconomic pathways. *Remote Sens* 15:2142. <https://doi.org/10.3390/rs15082142>
- Moré JJ (1978) The Levenberg-Marquardt algorithm: implementation and theory. In: Watson GA (ed) *Numerical Analysis*. Springer, Berlin, Heidelberg, pp 105–116
- O'Neill BC, Kriegler E, Riahi K, Ebi KL, Hallegatte S, Carter TR, Mathur R, van Vuuren DP (2014) A new scenario framework for climate change research: the concept of shared socioeconomic pathways. *Clim Change* 122:387–400. <https://doi.org/10.1007/s10584-013-0905-2>
- Pauliuk S, Arvesen A, Stadler K, Hertwich EG (2017) Industrial ecology in integrated assessment models. *Nat Clim Change* 7:13–20. <https://doi.org/10.1038/nclimate3148>
- Pittau F, Habert G, Savi D, Klingler M (2022) Carbon storage project. <https://www.research-collection.ethz.ch/handle/20.500.11850/554234>. Accessed 14 Feb 2025
- Popp A, Rose SK, Calvin K, Van Vuuren DP, Dietrich JP, Wise M, Stehfest E, Humpenöder F, Kyle P, Van Vliet J, Bauer N, Lotze-Campen H, Klein D, Kriegler E (2014) Land-use transition for bioenergy and climate stabilization: model comparison of drivers, impacts and interactions with other land use based mitigation options. *Clim Change* 123:495–509. <https://doi.org/10.1007/s10584-013-0926-x>
- Röck M, Saade MRM, Balouktsi M, Rasmussen FN, Birgisdottir H, Frischknecht R, Habert G, Lützkendorf T, Passer A (2020) Embodied GHG emissions of buildings – the hidden challenge for effective climate change mitigation. *Appl Energy* 258:114107. <https://doi.org/10.1016/j.apenergy.2019.114107>
- Roux C, Schalbart P, Peuportier B (2017) Development of an electricity system model allowing dynamic and marginal approaches in LCA – tested in the French context of space heating in buildings. *Int J Life Cycle Assess* 22:1177–1190. <https://doi.org/10.1007/s11367-016-1229-z>
- Sacchi R, Terlouw T, Siala K, Dirnaichner A, Bauer C, Cox B, Mutel C, Daioglou V, Luderer G (2022) PROspective EnvironMental Impact asSEment (premise): a streamlined approach to producing databases for prospective life cycle assessment using integrated assessment models. *Renew Sustain Energy Rev* 160:112311. <https://doi.org/10.1016/j.rser.2022.112311>
- Schmidt III R, Austin S (2016) *Adaptable Architecture*. Routledge
- Šimaitis J, Allen S, Vagg C (2023) Are future recycling benefits misleading? Prospective life cycle assessment of lithium-ion batteries. *J Ind Ecol* 27:1291–1303. <https://doi.org/10.1111/jiec.13413>
- Stehfest E, van Vuuren D, Bouwman L, Kram T (2014) Integrated assessment of global environmental change with IMAGE 3.0: model description and policy applications. Netherlands Environmental Assessment Agency (PBL)
- TOTEM (2021) Environmental profile of buildings. <https://www.totem-building.be/>. Accessed 10 Feb 2023
- UN Environment Programme (2024) Global status report for buildings and construction. <https://www.unep.org/resources/report/global-status-report-buildings-and-construction>. Accessed 11 Sep 2024
- Van de moortel E, Allacker K, De Troyer F, Schoofs E, Stijnen L (2022) Dynamic versus static life cycle assessment of energy renovation for residential buildings. *Sustainability* 14:6838. <https://doi.org/10.3390/su14116838>
- van Vuuren DP, Edmonds J, Kainuma M, Riahi K, Thomson A, Hibbard K, Hurtt GC, Kram T, Krey V, Lamarque J-F, Masui T, Meinshausen M, Nakicenovic N, Smith SJ, Rose SK (2011) The representative concentration pathways: an overview. *Clim Change* 109:5. <https://doi.org/10.1007/s10584-011-0148-z>
- van Vuuren DP, Riahi K, Calvin K, Dellink R, Emmerling J, Fujimori S, Kc S, Kriegler E, O'Neill B (2017) The shared socio-economic pathways: trajectories for human development and global environmental change. *Glob Environ Change* 42:148–152. <https://doi.org/10.1016/j.gloenvcha.2016.10.009>
- Voglhuber-Slavinsky A, Zicari A, Smetana S, Moller B, Dönitz E, Vranken L, Zdravkovic M, Aganovic K, Bahrs E (2022) Setting life cycle assessment (LCA) in a future-oriented context: the combination of qualitative scenarios and LCA in the agri-food sector. *Eur J Futur Res* 10:15. <https://doi.org/10.1186/s40309-022-00203-9>
- Zimmermann BM, Dura H, Weil M (2014) Towards time-resolved LCA of electric vehicles in Germany. *Metall Res Technol* 111(3):169–178. <https://doi.org/10.1051/metal/2014009>

**Publisher's Note** Springer Nature remains neutral with regard to jurisdictional claims in published maps and institutional affiliations.